Easy Scalable Avenue of Anti-bacterial Nanocomposites Coating Containing Ag NPs Prepared by Cryomilling

Nirmal Kumar Katiyar[a,b] and Krishanu Biswas[a*]

[a]*Department of Material Science & Engineering, Indian Institute of Technology Kanpur, Kanpur -208016 INDIA*

[b]*School of Engineering, London South Bank University, 103 Borough road, London, SE10AA*

Abstract

The antibacterial coating is required in many sectors such as water treatment plants, healthcare surfaces, air conditioners, doors, etc, and the process must be scalable for a low cost. An antibacterial agent in the coating endowed the antibacterial action of the coating and more extended durability. Therefore, metal nanoparticles are the best alternatives to antibiotics and other hazardous substances. The production of nanoparticles in mass and their distribution in the coatings is the biggest challenge yet. The cryomilling technique is known to be large-scale production of metal nanoparticles (NPs), and among the other metals, the Ag metal nanoparticles are the remarkable antibacterial agent. In addition, the sol-gel coatings are easy scalable for a large surface. Therefore, the pristine free standing Ag NPs were prepared by the cryomilling (milling at <123 K temperature) and *ex-situ* added in the silica-based SOL synthesized by silicon alkoxide hydrolysis and condensation. The Ag NPs embedded silica sol has been deposited over glass coverslips and aluminum panels using a dip-coating technique. They were characterized in coating stability, nanoparticles homogeneous distribution, and antibacterial/anti-fouling property against *Staphylococcus aureus* and *Escherichia coli* bacterial strains. The sol-gel nanocomposite coating embedded with free-standing Ag NPs has been found to exhibit excellent antifouling property against both the bacterial cell lines with the highest antibacterial efficiency of 92 and 90 % against *E.coli* and *S. aureus*, respectively.

Keywords: Cryomill, Antifouling, Antibacterial, Ag NPs, Large Scale, High purity, Sol-gel coatings

1) **E mail-** kbiswas@iitk.ac.in , **Phone - +91**-512-2596184, **Fax-+91**-512-2597505

1 Introduction

Nowadays, the industries and research academia are dealing with nanocomposites coating to enable the surface with tailored functionalities such as antibacterial/anti-fouling action[1-4], anti-corrosion[5], self-cleaning, super hydrophobicity[6], etc. The functional antibacterial coating over the surface reveals in almost all disciplines materials science, chemical science, nanotechnology, and biotechnology[7]. The antibacterial and anticorrosive coating have daily life use as well as industrial use. Thus, it is required an easily scalable and economical method for different industries such as water treatment, air conditioners, industrial equipment, healthcare surfaces and doors, vehicles, etc. Therefore, the nanocomposites hybrid coating is continuously developing to overcome such problems - an infection spread through different surfaces and growing bacterias in industrials plant surfaces, etc. The bacterial infection in daily life is a human life threat, and in industrials, undesired organism growth in economic loss such as fouling in ship hull[8, 9]. Bio-fouling is a serious problem for vehicles traveling in the marine environment for centuries [10, 11]. In general, this is defined as an unwanted accumulation of microorganisms on the wet surfaces of marine vehicles [11]. This problem has received tremendous attention in the last 50 years because of a large number of seaborne vehicles in the expanded trade routes. A detailed study indicates that bio-fouling has continuously increased at an alarming rate from the last few decades. Thus, this is recognized as a tremendous threat to the economy and the marine ecology. In order to mitigate this global problem, there have been intense research and development activities going on across the globe. In the 1960s, tributyltin (TBT) was widely utilized on the wet surface of marine vehicles [12, 13]. TBT was very effective against the fouling microorganisms. However, TBT was found to be highly poisonous for non-target micro-organisms, and its use on the external surfaces was completely banned in

2001 with an order to reduce the usages of toxic contamination in seawater to protect precious marine life [12]. Thus, the critical issue remains as to how to combating bio-fouling without putting our ecosystem on risk. After the prohibition on the use of tin-based coating, copper has emerged as the alternative antifouling release coatings. But, copper has also toxic nature to non-target sea microorganisms such as *Vibrio fischeri*, microalgae, *Ceramium tunicorne*, and *Harpactacoid copepod* etc. [13-15]. In fact, the high concentration of Cu^{2+} increases the risk, further causing adverse effects in the ambient aquatic life [16-18].

It has been proved beyond doubt that the metal nanoparticles based antibacterial coatings are the best alternative to combat antibacterial/bio-fouling in the literature[19-22]. However, one needs to choose a suitable metal, which will not lead to or reduce the toxicity to the non-target marine species while providing sufficient antibacterial properties. Considering these aspects, silver nanoparticles (Ag NPs) have exceptional antibacterial properties and non-toxic nature for non-target organisms[18, 23, 24]. The surface chemistry leading to the release of anti-fouling/antibacterial agents from the coating is the dominant factor for the adhesion of micro-organisms in the aqueous surrounding/environment and the existence of NPs on the surfaces subject to bacterial infection. Sol-gel silica-based coating with hydrophobicity has emerged as a good alternative for antibacterial/anti-fouling applications in large scale production. Karlsson *et al*. [25] have shown that silica-based coatings do not have toxic effects on non-target organisms and are easy to commercialize in small or large scale industries due to simplicity.

The extremely fine metal nanoparticle preparation on a large scale, their homogeneous dispersion in the coatings (non-agglomeration), and non-defective coating deposition are the biggest challenges. Therefore, a scalable metal nanoparticle preparation technique known as

cryomilling[26-29] has been utilized to prepare Ag NPs and *ex-situ* added in the silica-sol prepared by hydrolysis subsequent condensation of methyl group-containing silicon alkoxide. The coating has been deposited over the metal surfaces and the glass surface to characterize antibacterials action and any adverse effect of nanoparticle addition in the coating.

The present investigation reports the development of a unique foul release silica-based hybrid nanocomposite coating, containing nano-sized (6-10 nm) silver particles for anti-bacteria as well as anti-fouling applications. The article demonstrates the superior inhibitory efficiency of free-standing ultra-pure Ag NPs in sol-gel silica coating for antibacterial/anti-fouling activities towards *Staphylococcus aureus* (*S. aureus*) and *Escherichia coli* (*E. Coli)* bacterial cells.

2 Experiments

2.1 Materials

The silver powder (spherical, -325 mesh, 99.9%) from Alfa Acer USA has been used to prepare silver nanoparticles (Ag NPs). TEOS (Tetraethoxysilane and Octyltriethoxysilane (OTES)), MTES (Methyltriethoxysilane 98 wt%) received from GELEST Inc., USA for preparation of the sol. HIMEDIA ® supplied Luria Bertani Broth (LB) miller used as media for the cultivation of bacteria. Thiazolyl Blue Tetrazolium Bromide (SRL Ltd.) was utilized for the detection of bacterial cell viability.

2.2 Preparation of Free standing Silver NPs

The cryomilling process prepared the free-standing Ag NPs. The detail of the Ag nanoparticles preparation is mentioned elsewhere [27, 29, 30]. The custom-built cryomill has been used, whereas the mill was maintained below -160±10 ^{o} C temperature using LN_2 (liquid nitrogen).

The cryomill was designed so that the LN_2 and silver powder do not mix each other; a schematic of the cryomill is shown in Figure 1(a). Therefore, powder milling was always performed in a dry environment. The milling has been performed in the inert environment by continuously introducing Argon (Ar) gas in the milling chamber, and temperature measured using K-type thermocouple with NI9211 DAQ card (NI: National Instruments). The BPR (ball-to-powder ratio) of 80:1 was utilized for mechanical milling. The cryo-milled powder was dispersed in ethanol and found to free stand for sufficient time. The synthesized nano-powder was found to have ultra-high purity, and narrow sized particles with 97% yield having 34 ppb tungsten (W) come from the ball and vials as foreign substances, which is almost negligible[27]. Therefore, the cryomilling technique can produce a large amount of Ag NPs with the native surface. The details of the cryomilling advantages can be seen in previous studies[30-35]. Alternatively, other wet chemical techniques always have some surfactant or capping agents along with reducing agent and also suffer from lack of yield and shows toxicity.

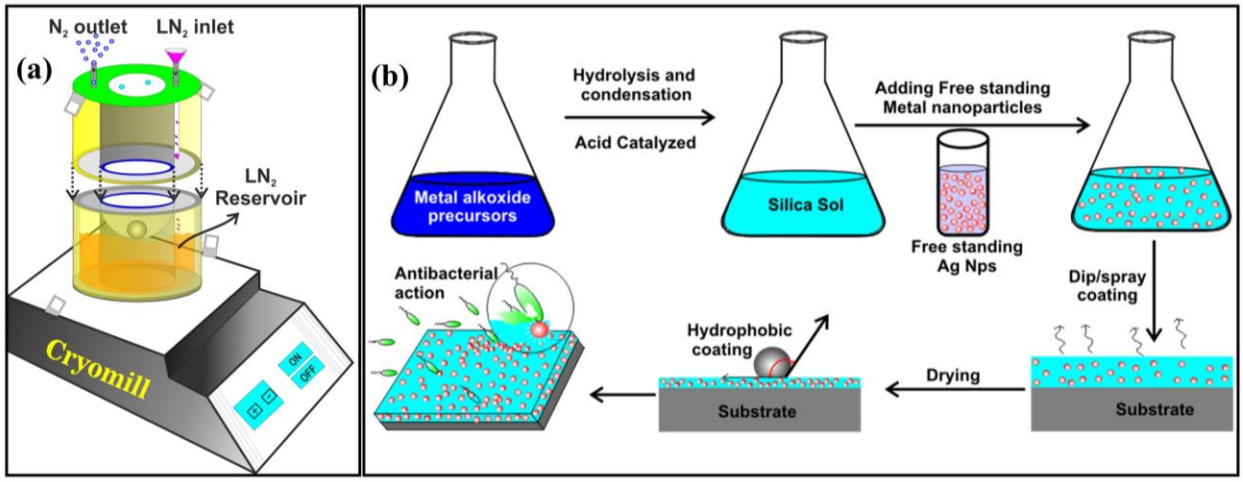

Figure 1: (a) schematic of cryomill **(b)** process overview of the synthesis of Ag NPs, embedded in the silica sol, and coating deposition.

2.3 Preparation of Sol

The sol was prepared using three types of alkoxysilanes- tetraethoxysilane (TEOS), methyltriethoxysilane (MTEOS), and octyltriethoxysilane (OTES) precursors. In the process, the alkoxides were hydrolyzed and condensed in the acidic medium using the molar ratio shown in Table 1. MTEOS and TEOS have been mixed along with a half quantity of ethanol in a reaction vessel in the first step. The 0.1 N HCl was mixed with water in a separate flask (acidified water). The half amount of the acidified water was added dropwise under vigorously stirring in the reaction vessel and left for 4 h. Afterward, OTES was mixed, and then the remaining acidified water was added dropwise. Finally, the overnight stirring was carried out for complete hydrolysis and condensation. The sol was ready and diluted further using ethanol. In the acidic conditions, the first step, an alkoxide group, is likely protonated. Therefore, the silicon atom becomes slightly positive. Thus, it becomes electrophilic and more susceptible to react with water[36]. The acidic condition supported fast hydrolysis and slow condensation, which ultimately led to the formation of functional three-dimensional networks (-O-Si-O-)n, as shown in Figure 2. Prior to the coating deposition, free-standing Ag NPs have been embedded in the sol in different quantities.

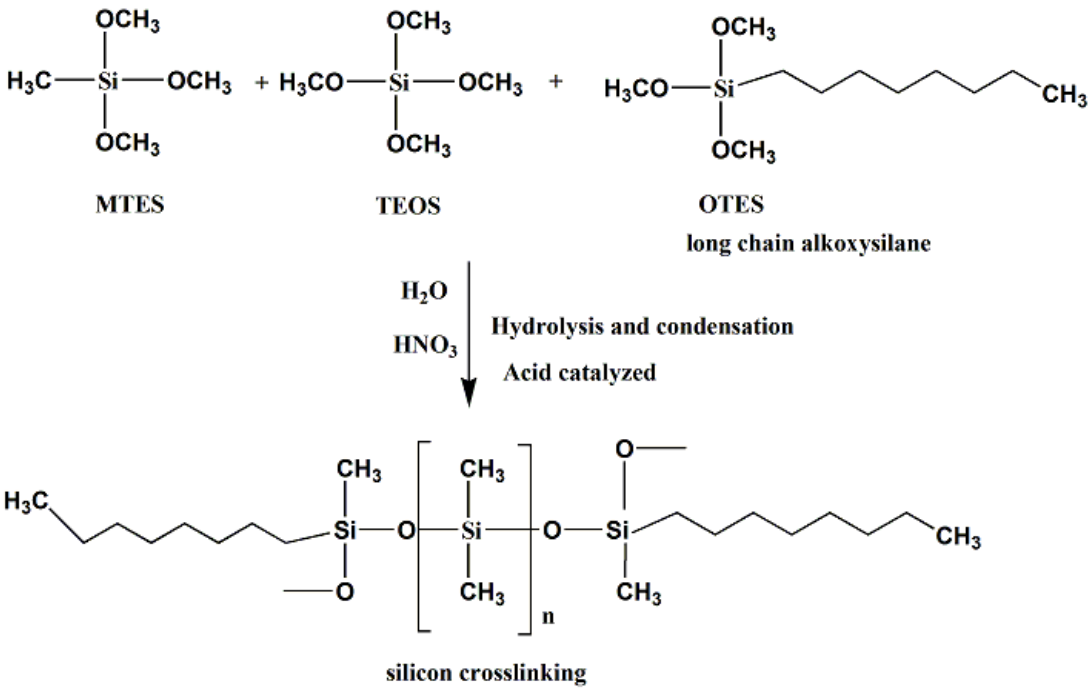

Figure 2: Acid-catalyzed hydrolysis and condensation reaction.

Table 1: A molar ratio of chemicals used for the preparation of sol

MTEOS	TEOS	EtOH	OTES	HCl	H_2O
3	1	12.7	1	0.25	8

2.3 Coating Deposition

The detail of the coating process schematic has been illustrated in Figure 1(b). The free-standing silver metal nanoparticles (dispersed in ethanol) were embedded in the as-prepared silica sol in varying concentrations such as 0, 0.04, 0.05, 0.055, 0.06, and 0.065 wt%. The coatings were deposited on the pure aluminum panels of 5 cm x 10 cm dimension (Q-lab Florida) using a dip

coater with a withdrawing rate of 0.3 cm/s. The coating was also deposited over glass coverslips for biological tests and cured at 200 ^{o}C for 2 h.

2.4 Characterization

The size and shape of silver nanoparticles have been investigated using a TEM (Transmission Electron Microscope) makes FEI, TITAN G^2 60, operated at 300 kV. The synthesized powder was dispensed in HPLC grade CH_3OH, followed by ultrasonication. One drop taken from the middle of the test tube using a micropipette disperse solution was placed over 400 mesh size carbon film containing the TEM grid. It was dried 12 hours before the analysis. The interaction of silver nanoparticles with the silica matrix was studied using XPS (X-ray photoelectron spectroscopy) make PHI 5000 Versa Prob II, FEI Inc. The binding energies charge correction with respect to adventitious C 1s peak 284.8 eV has been performed. The coating thickness was investigated using Filmetrics F20, USA, and the water contact angle with coating has been investigated using a Kruss Gmbh Germany contact angle instrument. The stability of coatings against saltwater was examined using a salt spray test according to ASTM B117 with 5 wt% NaCl solution at 35 ^{o}C as well as a dynamic polarization test. The potentials were varying from -1 V to +0.6 V with a step rate of 1mV/s, and the data were collected using a computer-controlled Solarton Electrochemical Interface (Model 1286). The recorded results were analyzed using CORRVIEW2 software. The leaching of Ag NPs from the coating was estimated using ICP-MS (Agilent technologies model 7900).

2.5 Bacterial Culture Test

The two bacterias, *E.* coli (MCC2079) and *S. aureus* (MCC2043) were obtained from NCCS (National Centre of Cell Science), Pune, India. Both bacterias were cultured in Luria Broth (LB)

medium and incubated overnight at 37°C. Further, the culture was used to streak over a freshly prepared agar plate. A single colony of bacteria was procured. The procured single colony of bacteria was used to culture/extend the bacteria using freshly prepared LB media in an incubator, temperature maintained at 37°C[37]. This pure suspension of each bacterial cell with 10^8 CFU/ml of medium set through optical density OD=0.5 at 600 nm was used to analyze in vitro bacterial experiments.

2.5.1 Determination of antibacterial efficacy

The Ag NPs embedded in silica-based sol-gel coatings were prepared with varying amounts of the NPs (0, 0.04, 0.05 0.055, 0.060, and 0.065 wt%). Coating with zero amounts of Ag NPs was considered control. Glass coverslips were used to deposit the biological tests coating. These samples were seeded with bacteria cells and incubated for 4 h at 37^o C. After incubation; the coated glass coverslips were correctly washed as per the protocol [38] and observed under SEM (FESEM, Nova Nano SEM 450).

2.5.2 Cytotoxicity assay (MTT)

The bacterial cytotoxicity analysis was performed via the reduction of the MTT reagent (3-[4,5-dimethyl-thiazol-2-yl]-2,5-diphenyltetrazolium bromide, Sigma)[39]. The dye (MTT) gets reduced to the blue-violet colored end product, known as formazan crystals, by the electron transport system of living bacteria. All the samples, kept in 24 well plates, were seeded with 200 µl of each bacterial suspension at 0.5 OD_{670} and incubated at 37°C for 4 h. After a stipulated time period of incubation, purple formazan crystals were dissolved in 200 µl DMSO (dimethylsulfoxide). The absorption by formazan crystal (coloured product) was quantified

spectrophotometrically in a 96-well ELISA microplate reader (Bio-Tek, EL×800) at 550 nm to determine the bacterial viability.

2.5.3 Determination of colony formation units (CFU)

The *E.coli* and *S. aureus* were used for CFU determination on solid agar plates. The 200 µl (10^5 cells/ml) of freshly grown bacterial suspension was added into the well plate containing Luria broth media and Ag NPs embedded sol-gel coated glass coverslip followed by incubation at 37°C, for 4 h. One drop of media diluted at 10^5 fold was spread on nutrient agar plates to obtain discrete colonies. After incubation at 37°C for 24 h on the agar plate, the numbers of CFU (colony forming units) were observed on the agar plate.

2.5.4 Viability of Bacteria (LIVE/DEAD assay)

The bacterial cells's viability, *E. coli*, and *S. aureus*, on the surface of Ag NPs embedded sol-gel coatings were examined by staining with a dye kit (LIVE/DEAD® *Bac*Light™ Bacterial Viability Kit, Invitrogen, Molecular Probes, L7012). Coating with zero amounts of Ag NPs was considered as control. The bacteria suspension of 10^5 cells/ml after immersion in broth at 37°C for 4 h, the samples were rinsed with distilled water. The bacterial cells were immune-stained using the combination dye 50 ml (propidium iodide (PI) and SYTO 9) for 15 min, and further analyzed under a fluorescence microscope (Nikon LV 100D, Japan). The viable and non-viable cells, stained with PI and SYTO 9, respectively, can be differentiated easily, viable cells green, and non-viable appear red under the fluorescence microscope.

2.5.5 Statistical Analysis

The quantitative data obtained from bacterial viability analysis (MTT assay) were performed in triplicates and expressed as mean ± standard deviation. The comparison on significant results difference was performed using Dunnett's C test, and Dunnett's t-test at 95% confidence level. The p-value at 0.05 was considered as statistically significant.

3 Results

3.1 Transmission electron microscopy analysis

The nanoparticles prepared by cryomilling can retain their native or pristine surface. Thus, they can be easily dispersed in polar solvents (electrostatically stabilized)[28, 32]. The ability of well dispersion of Ag NPs have been used to disperse in methanol-based silica sol. Therefore, before embedded in the coating and after embedded, the nanoparticles have been analyzed using a transmission electron microscope. The Ag NPs nanoparticles average size was found 8±3 nm, calculated using approximately 500 nanoparticles, as shown in Figure 3(a). The single nanoparticles HRTEM image reveals the pristine Ag NPs, shown in Figure 3(b-c), (FFT filtered image (Ag (111) has been marked, d=0.23 nm)). Further, the Ag NPs were homogeneously dispersed in the silica sol. After that, the sol was deposited over TEM grid and cured at 200 ^{o}C. The NPs are homogeneously distributed in the silica matrix as seen in Figure 3(d); coating embedded single particle is shown in Figure 3(e), and corresponding ring diffraction pattern can be seen in Figure 3(f). The prepared NPs can homogeneously embed in the sol-gel derived functional coating, and they are stable in the cured organic-inorganic hybrid sol-gel coatings.

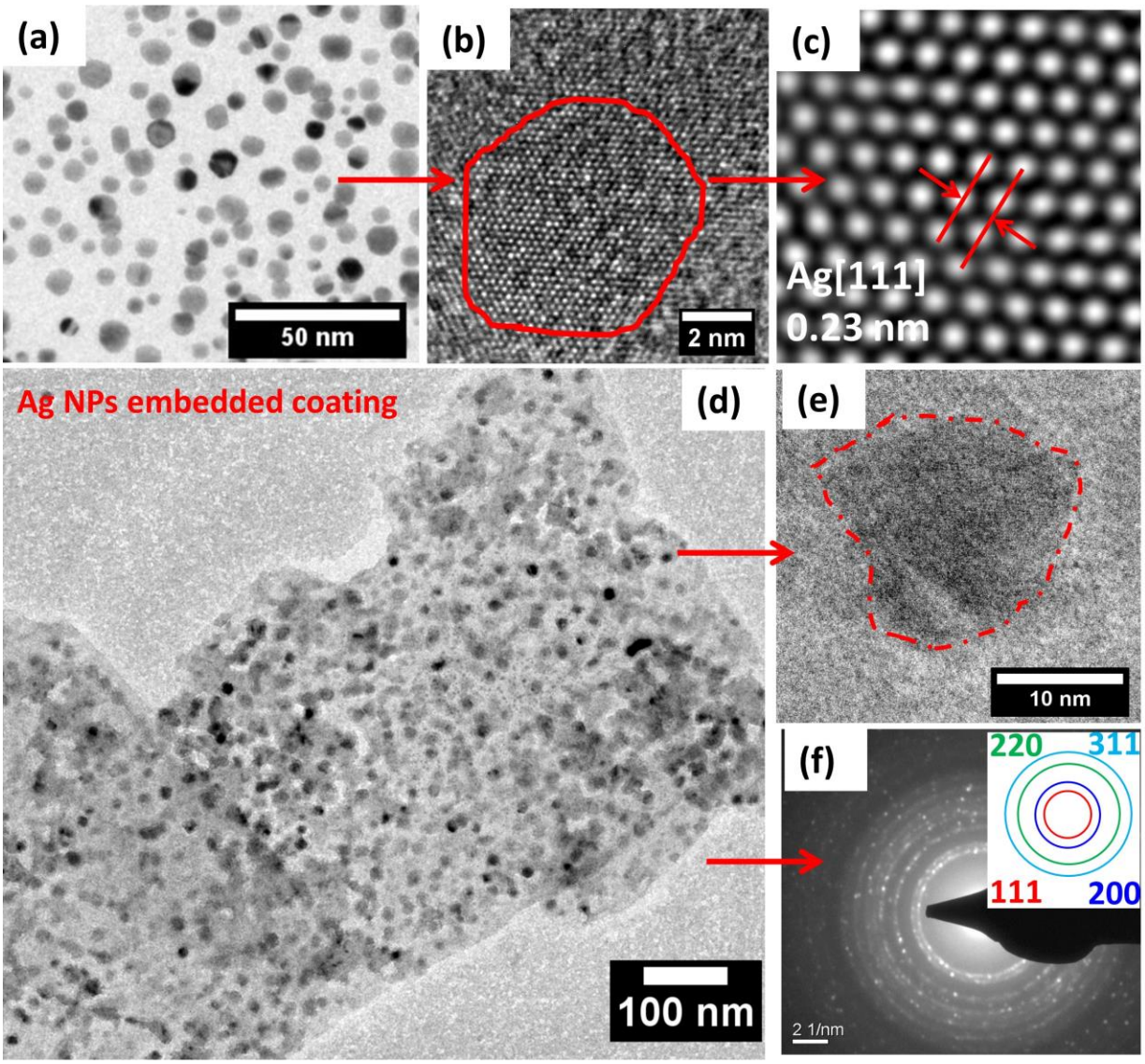

Figure 3: Transmission electron microscopy analysis of Ag NPs and embedded silica coating: **(a)** bright-field (BF) TEM image of Ag NPs; **(b)** HRTEM image of a nanoparticle **(c)** Fast Fourier Transform (FFT) filtered micrograph generated through the image (b); **(d)** TEM image of Ag NPs embedded silica coating; **(e)** TEM image of coating embedded single nanoparticles; **(f)** ring diffraction pattern corresponding to image (d).

3.2 X-ray photoelectron spectroscopy analysis

Sol-gel technique is one of the best synthesis methods to prepare coatings with embedded NPs [40, 41]. This can be either done by *in-situ* or *ex-situ* process. During *in-situ* synthesis, the nanoparticles are produced during sol preparation itself [20]. Contrary, in the *ex-situ* synthesis, the nanoparticles are prepared by some other method and later added to the sol. The critical aspect (irrespective of the *in-situ* or *ex-situ*), is the interaction of Ag NPs with the matrix. In the sol-gel process, two possible interactions are sol-gel entrapment and covalent attachment [42]. These types of interaction of NPs can influence nanoparticles' immobility, which can facilitate the antifouling action of the sol-gel coatings. Thus, it is essential to analyze the interaction between Ag NPs and the sol-gel coatings. Hence, the prepared coating has been analyzed by XPS. Figure 4(a-d) showed detailed XPS scans of C (1s), Si (2P), O(1s), Ag(3d), which indicated that the silica coating (0.065 wt % Ag NPs in Sol) consists of Ag NPs in the metallic form. Typically, the binding energy of Ag and AgO coincide, and it isn't easy to distinguish between the two[43-45]. However, the intense peak (368.12 eV) confirmed that the Ag NPs (Ag^0) were trapped in the functionalized silica network as an electrostatic entrapment. The broad peak, Si (2p) (102.4 eV), was a sign of a functionalized silica network as the corresponding oxygen bonding was observed in Figure 4(c). The presence of metallic silver is confirmed the electrostatic entrapment of NPs in sol-gel network, and porous coating can easily release the embedded Ag NPs and fulfill the desired properties.

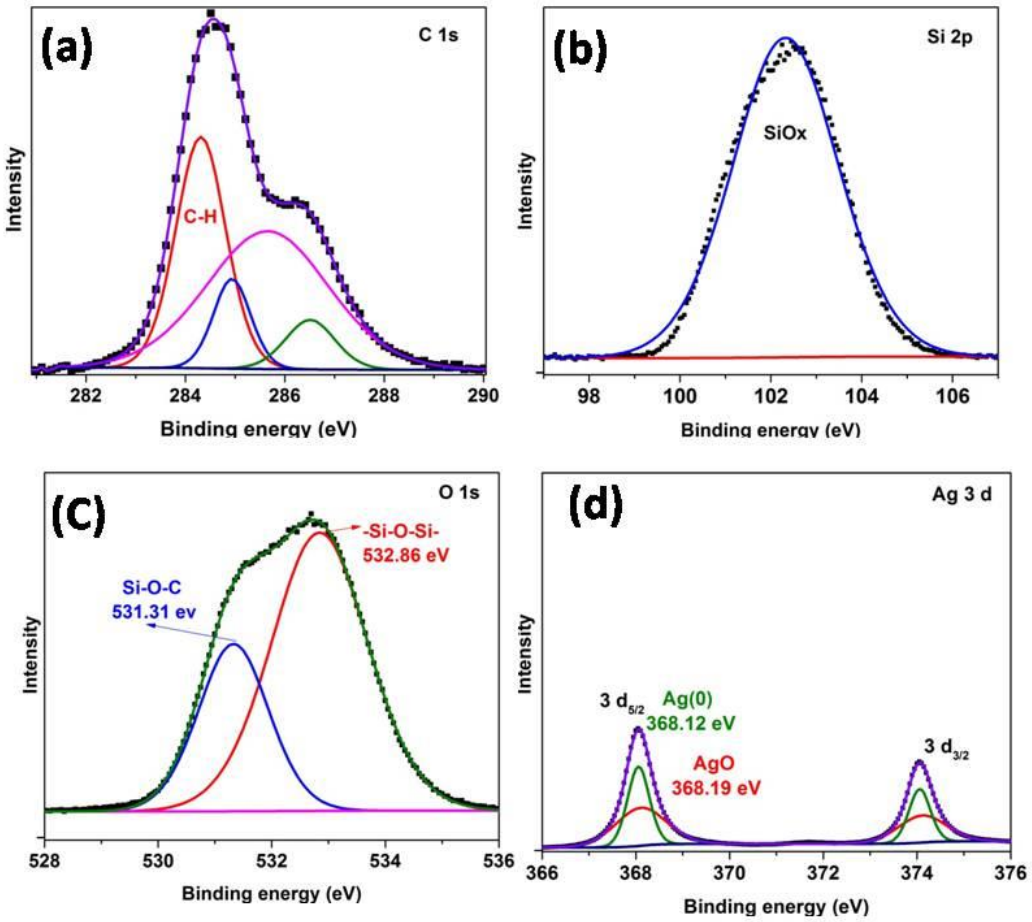

Figure 4: X-ray photoelectron spectroscopy spectra of Ag NPs embedded (0.06 wt%) silica coating on Al substrate: **(a)** C 1s; **(b)** Si 2p; **(c)** O 1s and **(d)** Ag 3d

3.3 Anticorrosive analysis

3.3.1 Salt spray

The salt spray is an accelerated corrosion initiation producing a corrosive attack on samples (similar to sea environment). Therefore, it mimics the sea environment and can be used to probe the surface's anticorrosive properties. The appearance of corrosion products is used to evaluate the stability of the film and the corrosion resistance property over a period of time. The sample

placed inside the chamber is tilted to expose its entire surface, with edges being covered with an adhesive tape.

Figure 5 shows the corrosion tested specimen's optical image to investigate the change in bare aluminum, silica-coated, and Ag NPs embedded silica-coated surfaces. It illustrates the condition of the samples after a week of the salt spray. The appearance of the photograph in Figure 5 (b and c) is similar. Therefore, the silica coating was highly durable in harsh environments, and Ag NPs were not causing any adverse effect on the coatings such as delamination and swelling. In contrast, coating retains its water contact angle 96°. On the other hand, the bare aluminum was vigorously corroded within 24 h [Figure 5 (a)]. After completion of exposure to salt spray, the samples have further been rinsed with deionized water and later analyzed using Field emission SEM. Figure 5 (d) showed that the bare aluminum was vigorously corroded, and the aluminum oxide layer would be peeled off to corrode further in-depth. In the case of the coated samples [Figure 5 (e)], there is no sign of any corrosion of coating after the salt spray test. Qualitatively, Ag NPs embedded silica coating reflects its anticorrosive suitability and durability in the harsh environment. Further, the anticorrosive property was analyzed using a potentiodynamic polarization test.

3.3.2 Potentiodynamic polarization analysis

The samples (bare, silica-coated, and Ag NPs embedded silica-coated) were exposed to N_2 gas purged 3.5 % NaCl solution for 1 h and 24 h. The results were analyzed using software named CORRVIEW2. The analyzed data are shown in Table 2. The corrosion current (i_{corr}) of the coated sample was one order lower than that of the bare substrate. The decrement in the open circuit potential (OCP), as also shown in Figure 5(f, g), might be the cause of the effective

suppression of the cathodic reaction of SiO_2 because it has a low IEP (isoelectric point) = 1.8 − 3.5. This allows it to develop a slightly negative surface charge (δ^-) at pH > 2. However, the coatings were immersed in the electrolyte solution of 3.5% NaCl with a neutral pH from 6.5 to 7, which is higher than the IEP, the OCP of the coated substrate was more negative compare to the bare substrate. The passive region is exposed (24 h) bare substrate was attributed to the oxide layer formation on aluminum surfaces. The silica-coated samples immersed for a longer time (24 h) showed a similar sharp passive region, clear evidence of the corrosion barrier (Figures 5f and 5g). It can be seen that though the corrosion resistance of the silica coating was higher than Ag NP embedded silica coating after 24 h exposure, still the corrosion resistance of the latter was higher than that of the bare aluminum substrate. The slight reduction in the barrier property of the Ag NPs embedded silica coating might be due to the embedded silver nanoparticles. However, the effect was not dramatic to cause a drastic change in the barrier properties. The coating is highly anti-corrosive as well as durable.

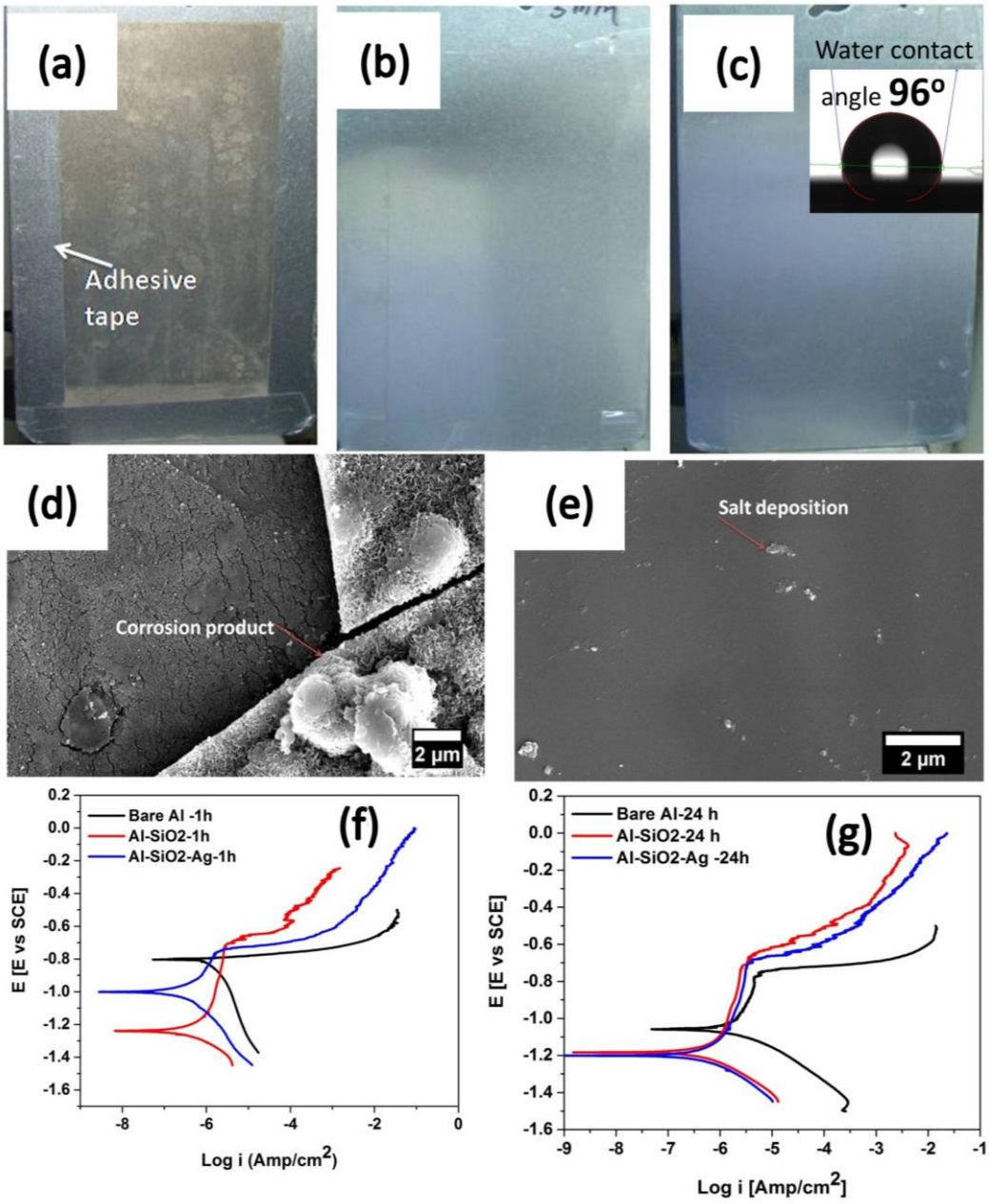

Figure 5: Optical image of salt spray tested specimens exposed for 144 hours: **(a)** Bare aluminium; **(b)** Silica coated; **(c)** 0.06 wt% Ag NPs doped silica coated; **(d)** FE-SEM micrograph of sample a; **(e)** FESEM image sample (c). Comparison of polarization data for bare aluminium, SiO_2 coated, and Ag NPs doped SiO_2 coated: **(f)** 1 h exposure; **(g)** 24 h exposure in 3.5 % NaCl solution.

Table 2: Summarized R_p fit results obtained from potentiodynamic polarization measurements

Sample Name	E_{corr} (Volts)	I_{corr}(Amp/cm^2)×10^{-7}	R_p (Ohms)
Bare Al-1 h	-0.8044	64.57	4071
Bare Al-24 h	-1.0494	16.03	16460
Al-SiO_2-1 h	-1.003	2.008	1.299E5
Al-SiO_2-24 h	-1.1826	3.992	65349
Al-SiO_2-Ag-1 h	-1.1356	1.555	1.677E5
Al-SiO_2-Ag-24 h	-0.8564	6.839	38140

3.4 Biological test (Antifouling on sol-gel coating)

The antifouling properties of the coating containing Ag NPs have been investigated by biological test, involving both qualitative as well as quantitative analysis.

3.4.1 MTT assay (quantitative analysis)

In the present study, the analysis of bacterial growth on the coating containing Ag NPs was investigated by determining the number of viable *E.coli* and *S. aureus* cells after contact with the samples for 4 h. The MTT assay was used to estimate the live bacterial growth inhibition, wherein optical density of the colored formazan crystal (viable bacterial cells produce formazan) was measured at A_{550} nm, and the results were expressed as percent inhibition, calculated using the following formula;

$$Percent\ of\ bacterial\ cells\ \ growth\ \ inhibition = \left(\frac{A_o - A_t}{A_o} \right) \times 100 \quad (1)$$

where A_o is the absorbance of the control (silver free) and A_t is the absorbance of Ag NPs embedded samples. Figure 6(a) showed the bacterial viability with varying concentrations of Ag NPs in the coating. The results are statistically determined to prove the significant difference ($p < 0.05$) using Dunnett's C and Dunnett's t-test. The Ag NPs at higher concentrations ($6.5x10^{-2}$ wt %) represent the highest growth inhibition efficiency of approximately 92 and 90 % for *E. coli* and *S. aureus* bacterial strains, respectively. In the MTT assay, only live bacteria can be estimated. Therefore, huge numbers of bacteria cells are grown in control. However, a dose-dependent decline in the proliferation of both the bacterial strains was observed on all the samples as Ag NPs concentration got increased. This test cannot distinguish between killing and inhibition of bacterial growth. The fouling is subjected to the attachment of bacteria on the surfaces, leading to biofilm formation in the aquatic environment [42]. But sol-gel coating does not allow easy attachment of bacteria with the surface due to its hydrophobic surface nature (water contact angle $96^o \pm 2$). Therefore, the embedded Ag NPs stimulate the inhibitory effects in bacterial growth.

3.4.2 FESEM (qualitative) analysis

The bacterial adhesions on coated glass coverslip (12 mm) were analyzed after 4 hours of incubation of the samples. Qualitatively, the bacteria density over the plate has been studied using FESEM. Figure 6(b, c) illustrates a fully grown *E.coli* colony over a silica-based sol-gel coated sample (Ag NPs free) with a high magnification image shown as an inset. On the other hand, the Ag NPs embedded in Sol-Gel coating reveals remarkably less colonization due to silver nanoparticles' release to the surface [Figure 6(c)]. A similar observation has also been

found in the case of *S. aureus* bacterial cells. These comprehensive analyses prove that the Ag NPs foul release sol-gel coating has high efficiency in combatting the fouling in ships, doors, medical-surgical appliances, etc.

3.4.3 Colony formation unit (CFU)

The efficiency of Ag NPs containing coating against the colony formation unit has been studied. Figure 6(f-i) shows the number of bacterial colonies grown on the nutrient agar plate, which signifies that the colony formation has been substantially reduced as the concentration of Ag NPs increases in the coatings. Therefore, the free-standing silver nanoparticle provides a better antifouling property. The +ve charged Ag ions from Ag NPs are considered to have attached to the -ve charged bacterial cell wall. As a result of its rupture, it is leading to the denaturation of proteins. This is the mechanism behind cell death or inhibition of bacterial cell growth [46].

3.4.4 Live/dead bacteria assay

The surface adhered viable and dead bacterias distribution on non-NPs embedded, and Ag NPs embedded coating after immersion in the bacterial suspension of 10^5 cells/ml for 4 h was observed via staining with the combination dye of PI and Syto9. The resulting fluorescence images are shown in Figure 6 (d-e). The results indicate that bacteria are viable after 4 h of incubation for control (silver free). But the samples with free-standing nanoparticles inhibit the growth of bacteria population, significantly reducing the growth of bacteria for both of the strains.

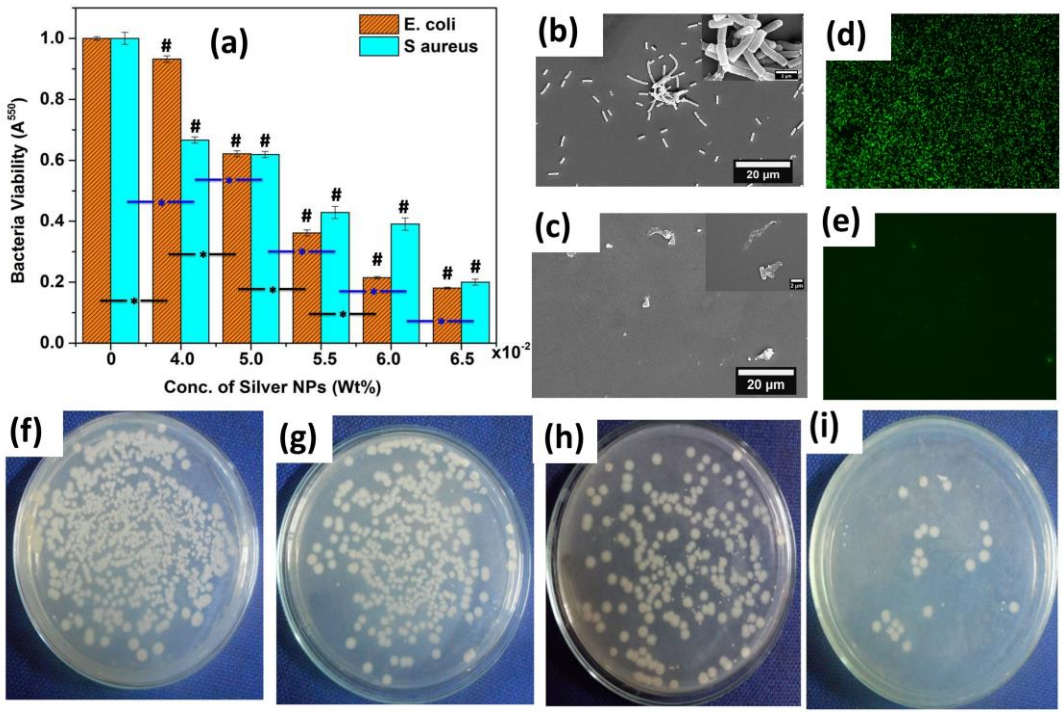

Figure 6: **(a)** MTT assay graph represents the bacterial cell viability against Ag NPs concentration after 4 h of incubation. Data are represented as average ± Standard deviation. The significant difference between the samples determined by Dunnett's C test, and a significant difference of the samples compared with the control sample determined by Dunnett's t test at a 95% confidence level. (* and # denote the mean difference significant at 0.05 level Dunnett's C and Dunnett's t test respectively); **(b)** FESEM image of *E.coli* bacteria after 4 h incubation, Ag-free silica-coated; **(c)** 0.06 wt % Ag NPs embedded silica-coated; **(d)** Live/dead bacteria viability fluorescence image of bacteria cells after 4 h of incubation *S. aureus* (control-silver free); **(e)** *S. aureus* with Ag NPs; **(f-i)** Digital photographs of *E. coli* bacteria colony grown over nutrient agar plate against concentration of embedded Ag NPs: **(f)** Control (silver free); **(g)** 0.05 wt %; **(h** 0.055 wt %; **(i)** 0.065 wt % of Ag NPs.

4 Discussion

The developed foul-release sol-gel organic-inorganic hybrid coating containing ultra pure free-standing Ag NPs is easily scalable. It serves the purpose of a good antibacterial/antifouling coating. The sol-gel coating's main attribute is the most straightforward technology of preparation and application over a large surface area of different aquatic and non-aquatic

surfaces. The silica-based coatings are easy to paint on steel [47], wood [48], fiberglass [49], or even aluminum. The associated properties of the coatings, such as hydrophobic nature, corrosion-resistant, and antibacterial effects, satisfy almost all the practical foul release coating requirements.

The coating has ethyl, methyl, and long-chain functional groups oriented on the surface, providing diversified coating properties [47]. The three types of silica alkoxide provide a highly cross-linked network, likely to accommodate Ag NPs in the matrix. Fundamentally, the presence of octyltriethoxy silane makes a complex robust crosslink with silica. The long organo-chain is chemically anchored and oriented towards the surface, providing long-lasting hydrophobic nature of the surface. There is no wetting of water and thus prevent the formation of biofilm.

In addition, the presence of ultra-pure, surfactant-free Ag NPs imparts excellent antifouling properties due to the migration of Ag NPs through the porous coatings affecting its surface property in the aquatic medium. In fact, Ag NPs do not act as a corrosion inhibitor or promoter in the long-lasting coating, which can provide antifouling properties for a longer duration. It is evident that the antifouling property of the Ag NPs is directly related to the selective release of the Ag NPs, when the coating comes in contact with seawater. To confirm this aspect, a fixed area of the coating was exposed to artificial seawater (3.5 wt% NaCl solution), and the concentration of leached Ag NPs was estimated using ICP-MS (detection limit~ 1part out of 10^{15} (ppq)). The results of the measurement are shown in Figure 7. It has been found that the released concentration of the coatings loaded with 0.06 wt% Ag NPs is 120 ppb/ml.cm^2 during the first 24 h and 200 ppb/ml.cm^2 after five days. Therefore, it demonstrates that Ag NPs got leached out slowly from the sol-gel coating, and hence, they were available on the surface for antifouling

action. It is to be noted here that the silica sol-gel has been prepared through acid-catalyzed reaction, and Ag NPs have been added *ex-situ*. Therefore, it is likely that Ag^{+} ions might also be present due to acid catalysis. This leads to a faster release of Ag NPs in the aquatic environment in the first 24 h of exposure, and later, the release has comparatively been reduced. However, the actual role of Ag NPs was favorable when the leaching was slow, and hence it provided longer antifouling property. The described foul release coatings could be treated as best suited for antifouling applications and easily scalable because Ag NPs can be produced in large quantity via cryo-milling, [29, 30].

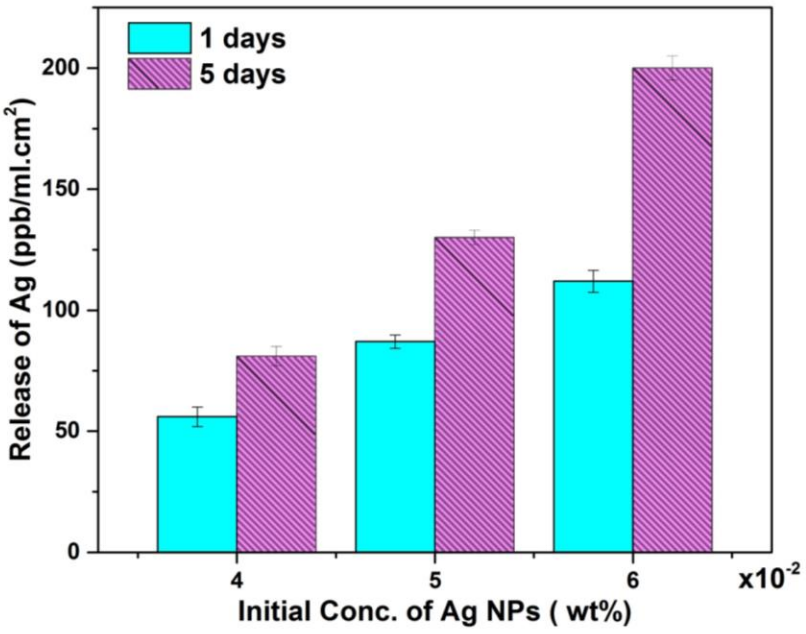

Figure 7: Concentration of the Ag in antifouling coating leaching out in artificial seawater within 1 and 5 days of period

Further, *in vitro* antibacterial study has demonstrated that incorporating nanoparticles Ag NPs in the presently designed coating can provide effective antibacterial action against *E.coli* and *S.*

aureus bacterial strains. These nanoparticles enhanced the antibacterial efficacy with 92 and 90 % of respective growth towards *E. coli* and *S. aureus*. Further, the antibacterial effectiveness of coating was also confirmed by the results obtained from FESEM, CFU, and live/dead assay. The present study categorically shows that the sol-gel coating is capable of inhibiting any possible attachment of bacteria due to Ag NPs as well as the hydrophobic nature of the silica coatings. In a nutshell, it suffices to state that the detailed analyses confirm that Ag NPs embedded in sol-gel silica coating can provide high efficiency to combat fouling in marine vehicles, and similar technologies can be applied to doors in the hospitals and surgical instruments, etc.

5 Conclusions

The foul-release sol-gel hybrid coating has immense importance in surfaces subjected to fouling or bacterial infection such as health care, air conditions, and industries equipment due to its superior antifouling and hydrophobic property well as corrosion resistance. This industrially scalable and cost-effective nature of the process makes it more usable for large surfaces, vehicles, and other medical appliances. The following conclusions can be made from the present study:

(a) The leaching of Ag NPs from coating was confirmed by estimation of Ag NPs concentration 200 ppb/ml.cm^2 in five days of aquatic exposure. The 24 h of exposure period resulted in the release of 120 ppb/ml.cm^{2,} which got decreased later. This behavior is beneficial for long-lasting antifouling/antibacterials properties.

(b) The synthesized standing Ag NPs were free from any ions or toxic reducing/capping agents, exhibiting their native properties.

(c) The prepared nanoparticles acted as a free stand in a polar organic solvent (methanol, ethanol, etc.), and the prepared silica sol was also found to be ethanol/methanol solvent-based. Therefore, NPs were easy to embed homogeneously in the silica matrix. The curing of sol-gel coating at low temperatures reduced the possibility of coarsening of Ag NPs. The Ag NPs did not show any adverse effect on coating properties, which is advantageous to this coating process.

(d) Moreover, coatings are extremely stable during the corrosion test. Such coatings exhibited 92 and 90 % growth inhibition of *E. coli* and *S. aureus,* respectively, as analyzed from various in vitro bacterial studies.

Finally, the present study's methods may serve as an efficient approach of utilizing free-standing cryo-milled Ag NPs or other metals in the silica sol to make superior antifouling coatings.

Acknowledgment

The author would like to acknowledge SERB-DST India for providing financial support for carrying out the present research work.

References

[1] E. Faure, C. Falentin-Daudré, T.S. Lanero, C. Vreuls, G. Zocchi, C. Van De Weerdt, J. Martial, C. Jérôme, A.-S. Duwez, C. Detrembleur, Functional Nanogels as Platforms for

Imparting Antibacterial, Antibiofilm, and Antiadhesion Activities to Stainless Steel, Adv. Funct. Mater, 22 (2012) 5271-5282, doi:https://doi.org/10.1002/adfm.201201106.

[2] J.Z. Soo, L.C. Chai, B.C. Ang, B.H. Ong, Enhancing the Antibacterial Performance of Titanium Dioxide Nanofibers by Coating with Silver Nanoparticles, ACS Appl. Nano Mater., 3 (2020) 5743-5751, doi:https://doi.org/10.1021/acsanm.0c00925.

[3] Z. Lin, X. Sun, H. Yang, The Role of Antibacterial Metallic Elements in Simultaneously Improving the Corrosion Resistance and Antibacterial Activity of Magnesium Alloys, Materials & Design, 198 (2021) 109350, doi:https://doi.org/10.1016/j.matdes.2020.109350.

[4] C. Zhao, L. Zhou, M. Chiao, W. Yang, Antibacterial hydrogel coating: Strategies in surface chemistry, Adv. Colloid Interface Sci., 285 (2020) 102280, doi:https://doi.org/10.1016/j.cis.2020.102280.

[5] X. Xu, D. Yi, Z. Wang, J. Yu, Z. Zhang, R. Qiao, Z. Sun, Z. Hu, P. Gao, H. Peng, Z. Liu, D. Yu, E. Wang, Y. Jiang, F. Ding, K. Liu, Greatly Enhanced Anticorrosion of Cu by Commensurate Graphene Coating, Adv. Mater., 30 (2018) 1702944, doi:https://doi.org/10.1002/adma.201702944.

[6] R. Yuan, S. Wu, P. Yu, B. Wang, L. Mu, X. Zhang, Y. Zhu, B. Wang, H. Wang, J. Zhu, Superamphiphobic and Electroactive Nanocomposite toward Self-Cleaning, Antiwear, and Anticorrosion Coatings, ACS Appl. Mater. Interfaces, 8 (2016) 12481-12493, doi:https://doi.org/10.1021/acsami.6b03961.

[7] M. Cloutier, D. Mantovani, F. Rosei, Antibacterial Coatings: Challenges, Perspectives, and Opportunities, Trends Biotechnol., 33 (2015) 637-652, doi:https://doi.org/10.1016/j.tibtech.2015.09.002.

[8] J.A. Callow, M.E. Callow, Trends in the development of environmentally friendly fouling-resistant marine coatings, Nat. Commun., 2 (2011) 244, doi:https://doi.org/10.1038/ncomms1251.

[9] M.S. Selim, S.A. El-Safty, M.A. Shenashen, S.A. Higazy, A. Elmarakbi, Progress in biomimetic leverages for marine antifouling using nanocomposite coatings, J. Mater. Chem. B, 8 (2020) 3701-3732, doi:https://doi.org/10.1039/C9TB02119A.

[10] X. Pei, Q. Ye, Development of Marine Antifouling Coatings, in: F. Zhou (Ed.) Antifouling Surfaces and Materials: From Land to Marine Environment, Springer Berlin Heidelberg, Berlin, Heidelberg, 2015, pp. 135-149.

[11] D.M. Yebra, S. Kiil, K. Dam-Johansen, Antifouling technology—past, present and future steps towards efficient and environmentally friendly antifouling coatings, Prog. Org. Coat., 50 (2004) 75-104, doi:http://dx.doi.org/10.1016/j.porgcoat.2003.06.001.

[12] S. Sonak, P. Pangam, A. Giriyan, K. Hawaldar, Implications of the ban on organotins for protection of global coastal and marine ecology, J. Environ. Manage, 90, Supplement 1 (2009) S96-S108, doi:http://dx.doi.org/10.1016/j.jenvman.2008.08.017.

[13] P.-Y. Qian, Y. Xu, N. Fusetani, Natural products as antifouling compounds: recent progress and future perspectives, Biofouling, 26 (2009) 223-234, doi:https://doi.org/10.1080/08927010903470815.

[14] E. Ytreberg, J. Karlsson, B. Eklund, Comparison of toxicity and release rates of Cu and Zn from anti-fouling paints leached in natural and artificial brackish seawater, Sci. Total Environ., 408 (2010) 2459-2466, doi:http://dx.doi.org/10.1016/j.scitotenv.2010.02.036.

[15] J.E. Gittens, T.J. Smith, R. Suleiman, R. Akid, Current and emerging environmentally-friendly systems for fouling control in the marine environment, Biotechnology Advances, 31 (2013) 1738-1753, doi:https://doi.org/10.1016/j.biotechadv.2013.09.002.

[16] C.L. Alzieu, J. Sanjuan, J.P. Deltreil, M. Borel, Tin contamination in Arcachon Bay: Effects on oyster shell anomalies, Mar. Pollut. Bull., 17 (1986) 494-498, doi:http://dx.doi.org/10.1016/0025-326X(86)90636-3.

[17] H. Okamura, I. Aoyama, D. Liu, R.J. Maguire, G.J. Pacepavicius, Y.L. Lau, Fate and ecotoxicity of the new antifouling compound Irgarol 1051 in the aquatic environment, Water Research, 34 (2000) 3523-3530, doi:http://dx.doi.org/10.1016/S0043-1354(00)00095-6.

[18] O. Bondarenko, K. Juganson, A. Ivask, K. Kasemets, M. Mortimer, A. Kahru, Toxicity of Ag, CuO and ZnO nanoparticles to selected environmentally relevant test organisms and mammalian cells in vitro: a critical review, Arch. Toxicol, 87 (2013) 1181-1200, doi:https://doi.org/10.1007/s00204-013-1079-4.

[19] D.M. Eby, H.R. Luckarift, G.R. Johnson, Hybrid antimicrobial enzyme and silver nanoparticle coatings for medical Instruments, ACS Appl. Mater. Interfaces, 1 (2009) 1553-1560, doi:https://doi.org/10.1021/am9002155.

[20] R. Procaccini, A. Bouchet, J.I. Pastore, C. Studdert, S. Ceré, S. Pellice, Silver-functionalized methyl-silica hybrid materials as antibacterial coatings on surgical-grade stainless steel, Prog. Org. Coat., 97 (2016) 28-36, doi:http://dx.doi.org/10.1016/j.porgcoat.2016.03.012.

[21] M.R. Detty, R. Ciriminna, F.V. Bright, M. Pagliaro, Environmentally Benign Sol–Gel Antifouling and Foul-Releasing Coatings, Acc. Chem. Res., 47 (2014) 678-687, doi:https://doi.org/10.1021/ar400240n.

[22] E.O. Ogunsona, R. Muthuraj, E. Ojogbo, O. Valerio, T.H. Mekonnen, Engineered nanomaterials for antimicrobial applications: A review, Applied Materials Today, 18 (2020) 100473, doi:https://doi.org/10.1016/j.apmt.2019.100473.

[23] C. Dowsett, The use of silver-based dressings in wound care, Nursing standard (Royal College of Nursing (Great Britain) : 1987), 19 (2004) 56-60.

[24] E.M. Hetrick, M.H. Schoenfisch, Reducing implant-related infections: Active release strategies, Chem. Soc. Rev., 35 (2006) 780-789, doi:https://doi.org/10.1039/b515219b.

[25] J. Karlsson, B. Eklund, New biocide-free anti-fouling paints are toxic, Mar. Pollut. Bull., 49 (2004) 456-464, doi:http://dx.doi.org/10.1016/j.marpolbul.2004.02.034.

[26] N.K. Katiyar, K. Biswas, C.S. Tiwary, L.D. Machado, R.K. Gupta, Stabilization of a Highly Concentrated Colloidal Suspension of Pristine Metallic Nanoparticles (Supporting Information), Langmuir, 35 (2019) 2668-2673, doi:https://doi.org/10.1021/acs.langmuir.8b03401.

[27] N. Kumar, K. Biswas, Fabrication of novel cryomill for synthesis of high purity metallic nanoparticles, Rev. Sci. Instrum., 86 (2015) 083903-083908, doi:https://doi.org/10.1063/1.4929325.

[28] N. Kumar, K. Biswas, Cryomilling: An environment friendly approach of preparation large quantity ultra refined pure aluminium nanoparticles, J. Mater. Res. Technol., 8 (2017) 63-74, doi:https://doi.org/10.1016/j.jmrt.2017.05.017.

[29] N. Kumar, K. Biswas, R.K. Gupta, Green synthesis of Ag nanoparticles in large quantity by cryomilling, RSC Advances, 6 (2016) 111380-111388, doi:https://doi.org/10.1039/c6ra23120a.

[30] N.K. Katiyar, K. Biswas, C.S. Tiwary, Cryomilling as environmentally friendly synthesis route to prepare nanomaterials, Int. Mater. Rev., (2020) 1-40, doi:https://doi.org/10.1080/09506608.2020.1825175.

[31] K. Barai, C.S. Tiwary, P.P. Chattopadhyay, K. Chattopadhyay, Synthesis of free standing nanocrystalline Cu by ball milling at cryogenic temperature, Mater. Sci. Eng. A., 558 (2012) 52-58, doi:https://doi.org/10.1016/j.msea.2012.07.059.

[32] N.K. Katiyar, K. Biswas, C.S. Tiwary, L.D. Machado, R.K. Gupta, Stabilization of a Highly Concentrated Colloidal Suspension of Pristine Metallic Nanoparticles, Langmuir, 35 (2019) 2668-2673, doi:https://doi.org/10.1021/acs.langmuir.8b03401.

[33] N. Kumar, C.S. Tiwary, K. Biswas, Preparation of nanocrystalline high-entropy alloys via cryomilling of cast ingots, J. mater. Sci., 53 (2018) 13411-13423, doi:https://doi.org/10.1007/s10853-018-2485-z.

[34] C.S. Tiwary, S. Kashyap, K. Biswas, K. Chattopadhyay, Synthesis of pure iron magnetic nanoparticles in large quantity, J. Phys. D, 46 (2013) 385001-385005, doi:https://doi.org/10.1088/0022-3727/46/38/385001.

[35] A. Verma, K. Biswas, C. Tiwary, A. Mondal, K. Chattopadhyay, Combined Cryo and Room-Temperature Ball Milling to Produce Ultrafine Halide Crystallites, Metall and Mat Trans A, 42 (2011) 1127-1137, doi:https://doi.org/10.1007/s11661-010-0490-1.

[36] C.J. Brinker, G.W. Scherer, CHAPTER 2 - Hydrolysis and Condensation I: Nonsilicates, Sol-Gel Science, Academic Press, San Diego, 1990, pp. 20-95.

[37] E.R. Au - Sanders, Aseptic Laboratory Techniques: Plating Methods, JoVE, (2012) e3064, doi:https://doi.org/10.3791/3064.

[38] R.I. Freshney, Cultureof animal cells, Wiley Blackwell, 6 (2010) 796.

[39] H. Wang, H. Cheng, F. Wang, D. Wei, X. Wang, An improved 3-(4,5-dimethylthiazol-2-yl)-2,5-diphenyl tetrazolium bromide (MTT) reduction assay for evaluating the viability of

Escherichia coli cells, J. Microbiol. Methods, 82 (2010) 330-333, doi:http://dx.doi.org/10.1016/j.mimet.2010.06.014.

[40] B.M. Novak, Hybrid Nanocomposite Materials—between inorganic glasses and organic polymers, Adv. Mater., 5 (1993) 422-433, doi:https://doi.org/10.1002/adma.19930050603.

[41] P. Innocenzi, H. Kozuka, Methyltriethoxysilane-derived sol-gel coatings doped with silver metal particles, J. Sol-Gel Sci. Technol., 3 (1994) 229-233, doi:https://doi.org/10.1007/bf00486561.

[42] I. Banerjee, R.C. Pangule, R.S. Kane, Antifouling coatings: Recent developments in the design of surfaces that prevent fouling by proteins, bacteria, and marine organisms, Adv. Mater., 23 (2011) 690-718, doi:https://doi.org/10.1002/adma.201001215.

[43] A.M. Ferraria, A.P. Carapeto, A.M. Botelho Do Rego, X-ray photoelectron spectroscopy: Silver salts revisited, Vacuum, 86 (2012) 1988-1991, doi:https://doi.org/10.1016/j.vacuum.2012.05.031.

[44] O. Akhavan, E. Ghaderi, Bactericidal effects of Ag nanoparticles immobilized on surface of SiO_2 thin film with high concentration, Curr. Appl. Phys., 9 (2009) 1381-1385, doi:http://dx.doi.org/10.1016/j.cap.2009.03.003.

[45] A. Babapour, B. Yang, S. Bahang, W. Cao, Low-temperature sol-gel-derived nanosilver-embedded silane coating as biofilm inhibitor, Nanotechnology, 22 (2011), doi:https://doi.org/10.1088/0957-4484/22/15/155602.

[46] P. Pourali, M. Baserisalehi, S. Afsharnezhad, J. Behravan, R. Ganjali, N. Bahador, S. Arabzadeh, The effect of temperature on antibacterial activity of biosynthesized silver nanoparticles, BioMetals, 26 (2013) 189-196, doi:https://doi.org/10.1007/s10534-012-9606-y.

[47] N. Kumar, A. Jyothirmayi, K.R.C. Soma Raju, R. Subasri, Effect of functional groups (methyl, phenyl) on organic-inorganic hybrid sol-gel silica coatings on surface modified SS 316, Ceramics International, 38 (2012) 6565-6572, doi:https://doi.org/10.1016/j.ceramint.2012.05.040.

[48] R. Subasri, G. Reethika, K.R.C. Soma Raju, Multifunctional sol-gel coatings for protection of wood, Wood Mater. Sci. Eng., 8 (2013) 226-233, doi:https://doi.org/10.1080/17480272.2013.834967.

[49] L. Sowntharya, R. Subasri, A comparative study of different curing techniques for SiO_2-TiO_2 hybrid coatings on polycarbonate, Ceramics International, 39 (2013) 4689-4693, doi:https://doi.org/10.1016/j.ceramint.2012.11.045.